

# Self-Supervised Domain Calibration and Uncertainty Estimation for Place Recognition

Pierre-Yves Lajoie, Giovanni Beltrame

**Abstract**—Visual place recognition techniques based on deep learning, which have imposed themselves as the state-of-the-art in recent years, do not generalize well to environments visually different from the training set. Thus, to achieve top performance, it is sometimes necessary to fine-tune the networks to the target environment. To this end, we propose a self-supervised domain calibration procedure based on robust pose graph optimization from Simultaneous Localization and Mapping (SLAM) as the supervision signal without requiring GPS or manual labeling. Moreover, we leverage the procedure to improve uncertainty estimation for place recognition matches which is important in safety critical applications. We show that our approach can improve the performance of a state-of-the-art technique on a target environment dissimilar from its training set and that we can obtain uncertainty estimates. We believe that this approach will help practitioners to deploy robust place recognition solutions in real-world applications. Our code is available publicly: <https://github.com/MISTLab/vpr-calibration-and-uncertainty> *Index Terms*—Place Recognition, Uncertainty Estimation, Simultaneous Localization And Mapping

## I. INTRODUCTION

VISUAL Place Recognition (VPR) remains one of the core problems of autonomous driving and long-term robot localization. Recognizing previously visited places is essential for decision-making, to reduce localization drift in Simultaneous Localization and Mapping (SLAM), and to improve robots’ situational awareness in general [1]. While VPR techniques based on deep learning can achieve very high levels of accuracy on standard datasets [2], domain generalization is still a major concern when the deployment environment is visually and/or structurally different from the training data. The problem of domain discrepancies is especially important for indoors or subterranean deployments since most popular approaches are trained using GPS data on city streets images [3]–[5].

Generalization and feature transferability from one domain to another, are common issues in deep learning [6]. The most common and effective approach is still to calibrate or fine-tune, the representation to the testing domain. Given that most robots are deployed in known domains (e.g. roads, warehouses, etc.), one can refine the network using additional labeled samples directly from the known testing environment to tailor the representation to the target domain. While an effective

approach, the data labelling necessary to obtain new training samples can be prohibitively expensive in practice.

To solve this problem, we believe that robust SLAM can be used as a self-supervised tool for data mining in any environment without the need for external sensors or ground truth information. In standard SLAM, place recognition errors are known to cause catastrophic localization failures. However, recent progress in robust state estimation has shown that such erroneous VPR matches can be detected and removed during pose graph optimization (PGO) [7], [8]. In other words, robust PGO leverages the 3D structure of the environment and robot trajectory to classify VPR matches as correct and incorrect. Both correct and incorrect matches can in turn be used to fine-tune VPR networks to improve their performance or obtain uncertainty estimates.

Therefore, in this paper, we propose a self-supervised domain calibration approach to extract new training samples from any target domains and improve VPR networks accuracy. In addition, we propose a technique to train an uncertainty estimator for place recognition using the new extracted samples.

First, we show that our self-supervised approach to gather training samples can be used to train a VPR network from a pretrained classification model and achieve reasonable performance, thus demonstrating the strength of our self-supervised training signal. We then show that our approach can improve the performance of existing VPR solutions when applied to environments that are visually different from their training domain, as well as providing uncertainty estimates.

Previous self-supervised approaches [3], [9] relied on GPS localization to extract training samples from datasets by selecting images with minimal distance. However, this is not suitable for GPS-denied environments such as indoor, underwater or underground. Also, contrary to techniques using structure-from-motion (SfM) for data mining [10], our approach leverages additional outlier samples identified with robust SLAM to further improve the VPR network. Moreover, our approach is able to extract samples in any environment in which odometry estimates can be obtained, leveraging sensors such as IMUs and wheel encoders that are not used in SfM.

Our approach offers practical benefits for the deployment of VPR systems in real applications: it could be used to collect correct and incorrect training samples from a single calibration run through an environment similar to the target domain, or could be employed online for lifelong learning/tuning directly on the target environment. After calibration, the VPR network is able to detect more correct matches and identify uncertain images. Moreover, by producing fewer incorrect matches, it reduces the expensive computational burden of processing and

This work was partially supported by a Canadian Space Agency FAST Grant and a Vanier Canada Graduate Scholarships Award.

Department of Computer and Software Engineering,  
Polytechnique Montréal, Montreal, Canada,

{pierre-yves.lajoie, giovanni.beltrame}@polymtl.ca

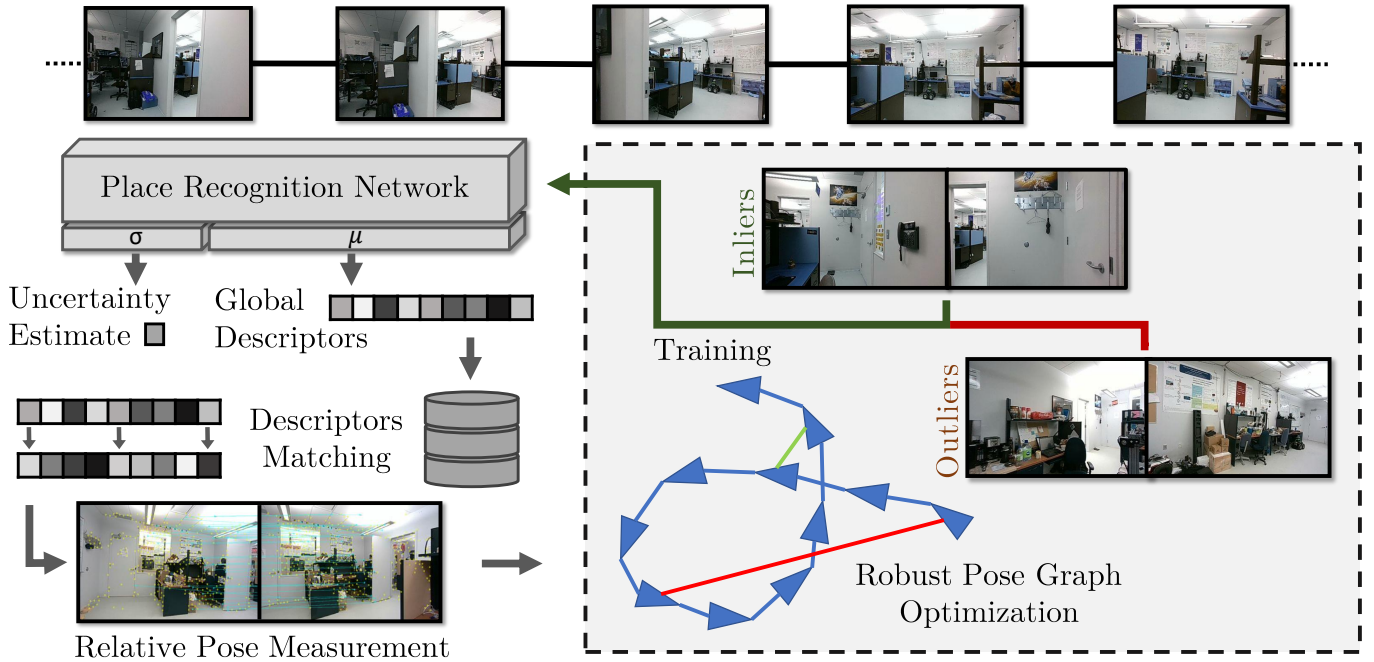


Fig. 1: **Self-Supervised Domain Calibration and Uncertainty Estimation via Robust SLAM:** Using a single calibration sequence through a new environment, our proposed self-supervised technique for visual place recognition verifies putative loop closures using recent progress in robust pose graph optimization, and uses both the resulting inliers and outliers to fine-tune the place recognition network. The place recognition network tuned to the new domain achieves better performance on subsequent sequences in visually similar environments, and provides uncertainty estimates tailored to those environments. Our calibration approach does not rely on GPS or any ground truth information, and can thus improve place recognition systems in any environment.

rejecting them [11]. Our contributions can be summarized as follows:

- A self-supervised training samples extraction method that does not require any external sensor (e.g. GPS), ground truth or manual labelling;
- A VPR sample classification method in correct and incorrect matches based on robust SLAM estimates;
- A domain calibration procedure for existing VPR techniques to improve their performance on any target environment using both correct and incorrect samples.
- An uncertainty estimator leveraging the new correct and incorrect samples during training;
- Open-source packages for sample extraction, network refinement and uncertainty estimation.

In the rest of this paper, Section II presents some background knowledge and related work, Section III details the proposed approach, Section IV demonstrate the effectiveness of the technique, and Section V offers conclusions and discusses future work.

## II. BACKGROUND AND RELATED WORK

### A. Visual Place Recognition

The ability to recognize places is crucial for localization, navigation, and augmented reality, among other applications [12]. The most popular approach is to compute and store global descriptors for each image to match, followed by an image retrieval scheme using a database of descriptors. Global descriptors are usually represented as high-dimensionality

vectors which can be compared with simple distance functions (e.g. Euclidean or cosine distance) to obtain a similarity metric between two images. The seminal work of NetVLAD [3] extracts descriptors using a CNN and leverages Vectors of Locally Aggregated Descriptors [13] to get a representation well-suited for image retrieval. The descriptor network is typically trained using tuples of images mined from large datasets. An anchor image is first chosen, then positive and negative samples are selected based on close and far GPS localization, respectively. A triplet margin loss pushes the network to output similar representations for positive and anchor samples and dissimilar representations for negative ones. Recent work has extended the concept of global descriptors by extracting local-global descriptors from patches in the feature space of each image [4]. In another line of work, [5] proposed a Generalized Contrastive loss (GCL) function that relies on image similarity as a continuous measure instead of binary labels (i.e., positive and negative samples).

Recent works in place recognition have aimed at computing uncertainty estimates for individual samples (i.e., images) using an uncertainty-aware loss during training [14]–[16]. This loss function allows the system to reduce its confidence and the priority of samples with high uncertainty. Similar to standard place recognition, the uncertainty estimates are dependent on the training domain, meaning it is beneficial to train those estimates on the target domain. In this work, we use the Bayesian Triplet Loss from [15] for correct samples and a Kullback-Leibler divergence loss for incorrect samples as described in Section III-D.

## B. Robust SLAM

In SLAM, place recognition is used to produce loop closure measurements between the current pose (i.e., rotation and translation) of a robot and the pose corresponding to the last time it has visited the place. Loop closure measurements are combined with odometry (i.e., egomotion) measurements in a graph representing the robot/camera trajectory. In other words, the SLAM algorithm builds a pose graph with odometry links between subsequent poses and loop closure links between recognized places. Pose graph optimization is then performed to reduce the localization drift of the robot [17]. When using a global descriptor method, such as NetVLAD, VPR serves as a first filter through potential matches, which is followed by the more expensive task of feature matching and registration to obtain the relative pose measurement corresponding to the loop closure. Due to the occurrence of perceptual aliasing (i.e., when two distinct similar-looking places are confused as the same), some loop closure measurements are incorrect and, if left undetected, they can lead to dramatic localization failures [7]. This phenomenon is particularly important when computing loop closures between multiple robots maps for collaborative localization [18].

To mitigate the negative effect of incorrect loop closure measurements during pose graph optimization, several approaches have been proposed. They vary from adding decision variables to the optimization problem [7], to leveraging clusters in the pose graph structure [19]. For the purpose of this paper, we chose a recent approach based on Graduated Non-Convexity which as been shown to efficiently achieve superior results [8].

It is important to note that these approaches allow us indirectly to classify loop closure measurements, and by extension also VPR matches, as correct (inliers) or incorrect (outliers).

## C. Domain Calibration

The goal of domain calibration is to improve the performance of a system on a target domain that is different from the training domain. This can be done through fine-tuning the model using samples from the target domain or through more complex domain adaptation approaches to enhance the generalization ability of the model. Domain calibration is also a major concern for long-term visual localization in changing environments. As presented in [20], one approach is to store multiple maps of the same environment to account for scene variation. To ensure the scalability, [21] proposes to summarize the maps, and [22], [23] suggest the use of compressed or coarse representations based on Hidden Markov Models.

Our approach could be used to adapt the VPR network to appearance changes. In fact, approaches in that line of research have been proposed for sequence adaption to cope with changing weather conditions during long-term missions [24], [25].

Interestingly, the exploitation of local feature patterns has been identified as a key to domain adaptation since they are more generic and transferable than global approaches [26]. Alternatively, recent work have proposed to include geometric and semantic information into the VPR latent embedding representation for visual place recognition [27] to better adapt to the target domain. In another line of work, [28] uses

temporal and feature neighborhoods in panoramic sensor data to mine training samples for VPR fine-tuning: they classify samples as correct using geometric verification, as opposed to our work where we leverage recent progress in robust SLAM.

Unlike related techniques based on GPS data [9], our approach is suited to any environment in which an odometry system (i.e., visual inertial odometry, lidar-based odometry paired with VPR, etc.) can be deployed, such as indoors, subterranean, or underwater. Our approach also requires significantly less data than SfM-based approaches [10]. Moreover, we include incorrect matches corresponding to loop closing outliers in the learning process to avoid such occurrences in the improved network. In addition, by adding an uncertainty head to the VPR network and using a Bayesian Triplet Loss [15], we are able to train an estimator for the heteroscedastic aleatoric uncertainty [29] (i.e., uncertainty corresponding to a particular data input) using only the extracted samples.

## III. SELF-SUPERVISED DOMAIN CALIBRATION AND UNCERTAINTY ESTIMATION

The main challenge addressed by our method is to extract pseudo-ground truth labels for training images. To tune the model to the target domain, we need to gather positive and negative place recognition matches from a single preliminary run through the environment. The classic approach is to use external positioning systems (e.g. GPS) to identify images that were captured in the same location as positive samples and images captured in distant locations as negative samples [3], [9]. We aim to extend this data mining scheme to any environment, regardless of the availability of ground truth localization. Our process is split in three sequential steps. First, we perform SLAM on an initial run through the target environment with a camera, or robot. In particular, we compute visual odometry, and we gather putative VPR matches from an initial network that was not tuned to the specific environment. Second, we sort the putative matches as correct or incorrect samples using robust pose graph optimization. Third, we use all the resulting samples to fine-tune the VPR network to the target domain and train an uncertainty estimator. A summary of the method is illustrated in Fig. 1.

### A. Finding VPR Matches

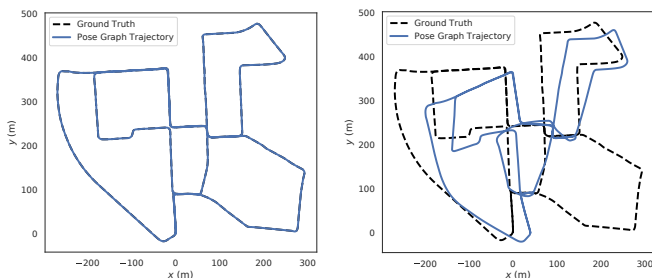
Global images descriptors can be complex structures such as Vector of Locally Aggregated Descriptors [13], used in NetVLAD [3], or simply the features extracted from the penultimate layer of a standard classification network [30]. The descriptors are represented as a vector  $f(I_i)$ , where  $f$  is the image representation extraction function and  $I_i$  the  $i_{th}$  keyframe. As keyframes are processed, we store the computed global descriptors in a database. Then, for each keyframe we query the best matches using nearest neighbors search, by sorting the global descriptors based on the Euclidean distance  $d(q, I_i)$  between the query descriptor  $f(q)$  and the other images descriptors  $f(I_i)$ . This results in a sorted list of the best putative VPR matches for each keyframe for the run through the environment. To avoid trivial matches in the same location, we do not consider matches with keyframes in the vicinity of the query.

## B. Classifying Matches

To filter the VPR matches, we first compute the relative pose between the pairs of images and integrate this information, as loop closures, in the SLAM pose graph. For each keyframe, we compute the relative pose between itself and the first image in its associated list (the best match). If we are able to successfully compute a relative pose measurement (i.e., loop closure), we store the two images as a (anchor, positive) training sample. Otherwise, we repeat the process with the next best match in the list. To obtain the negative samples, we go through the remaining best VPR matches in the sorted list and select up to  $N$  images for which a loop closure cannot be computed due to a lack of keypoint correspondences.  $N$  is set according to the available GPU memory for training. This way, we ensure that we extract the negative samples that appear the most similar to the anchor, yet that are not sufficiently similar to compute a loop closure. In other words, we select the most valuable negative samples for training, since they represent invalid VPR matches made by the uncalibrated network. This results in training tuples (1 anchor, 1 positive,  $N$  negatives) for each keyframe in the sequence.

Given the possible occurrence of perceptual aliasing, the computability of a relative pose measurement between the current anchor and positive frames, is not enough to guarantee that it is a correct place recognition match (see Fig. 2). Thus, we add the computed relative pose measurements to the SLAM pose graph as a loop closure and perform robust estimation using the Graduated Non-Convexity method [8].

From the resulting optimized pose graph, we can compute the error associated with every measurement and classify the VPR matches as correct or incorrect. A large error means that the match is in contradiction with the geometric structure of the pose graph and therefore incorrect. We then sort the measurements into the subsets of training samples  $S_{correct}$  and  $S_{incorrect}$ . The two subsets will be used with different loss functions during training.



(a) With correct loop closures (b) With 1 incorrect loop closure

Fig. 2: Illustration of the resulting KITTI00 pose graphs with and without an incorrect loop closure. We can see the large negative effect of even a single incorrect measurement on the localization accuracy. This motivates the need to detect such incorrect VPR matches using robust pose graph optimization. Those incorrect matches correspond to some of the most confusing parts of the environment and can thus be used in training to further improve VPR networks.

## C. Domain Calibration

The domain calibration of our VPR network is done through fine-tuning using the filtered training tuples in the tuning sets. In other words, starting from the pretrained network, we performed additional training iterations using the extracted data.

For the subset of correct samples, we applied the triplet margin loss  $L$  for each training tuple  $(q, p^q, \{n_i^q\}) \in S_{correct}$ ,

$$L = \sum_i \max(d(q, p^q) + m - d(q, n_i^q), 0) \quad (1)$$

where  $m$  is the margin,  $q$  is the global descriptor of the query image,  $p^q$  is the global descriptor of the positive image associated with the query, and  $n_i^q$  are the corresponding negative samples descriptors. The global descriptors are  $1 \times K$  vectors resulting from a forward pass through the VPR network and the distance function  $d$  is the Euclidean distance between the vectors. This strategy is analog to the training method used in NetVLAD [3].

On the other hand, the incorrect samples  $S_{incorrect}$  are composed of only one query and one negative images  $(q, n^q)$  and do not contain a positive image  $p$  such that we cannot use the triplet margin loss. Therefore, for each incorrect sample, we use a negative *Mean Squared Error* loss to increase the distance between the corresponding descriptors,

$$L = -\frac{1}{K} \sum_k (q_k - n_k^q)^2 \quad (2)$$

At each epoch we train on both correct and incorrect samples.

## D. Uncertainty Estimation

To learn an estimator tuned to the desired target environment, we follow [15] and add an uncertainty head to the baseline CNN network composed of a Generalized Mean (GeM) layer [10] followed by two fully connected layers with a softplus activation function. The resulting network has two outputs, a mean  $\mu$  and a variance  $\sigma$ , such that it encodes the descriptors as isotropic Normal distributions  $\mathcal{N}(\mu, \sigma)$  instead of point estimates.

For each correct sample, the uncertainty-aware loss computes the probability that the query  $q$  is closer to a positive  $p$  than a negative  $n$  given a margin  $m$ , and a prior  $1/K$  for normalization,

$$P(\|q - p\|^2 < \|q - n\|^2 - m), \quad (3)$$

For incorrect samples, we use instead the Kullback-Leibler divergence  $D_{KL}(V||T)$  loss between the descriptors distribution estimates ( $V \in \mathcal{N}(\mu, \sigma)$ ) and a target high variance distribution with the same mean ( $T \in \mathcal{N}(\mu, \sigma_{high})$ ) for which we have set the variance  $\sigma_{high}$  to  $H$  times the prior. A higher  $H$  increases the incorrect matches loss and thus their importance during training. For isotropic Normal distributions,  $D_{KL}(V||T)$  is defined as follows [32],

$$D_{KL}(V||T) = \frac{1}{2} \left( \log \frac{\sigma_{high}^2}{\sigma^2} + \frac{\sigma^2}{\sigma_{high}^2} - 1 \right) \quad (4)$$

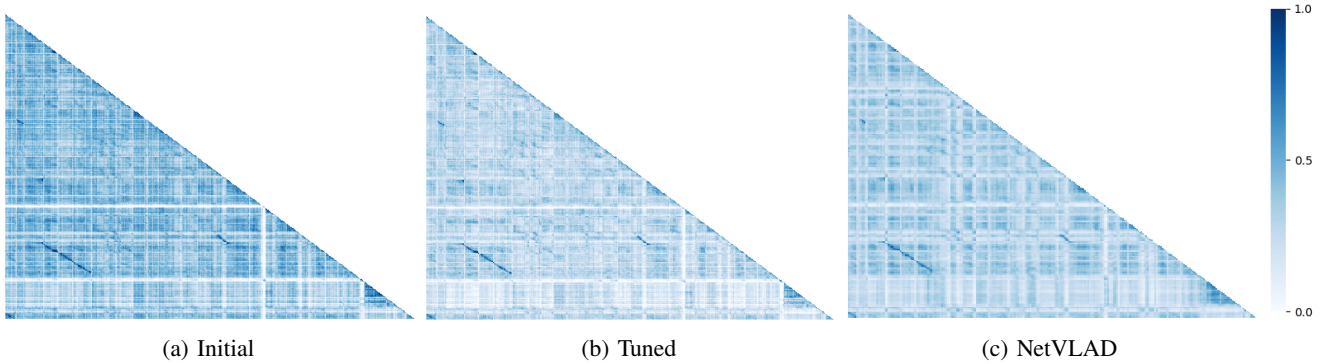


Fig. 3: Self-Supervised learning of a visual-similarity metric. An illustration of the similarity matrix before (Initial) and after (Tuned) training compared with the similarity obtained from NetVLAD on the KITTI-00 sequence. As expected, the similarity between positive pairs has increased (blue), and it has decreased between negative pairs (white).

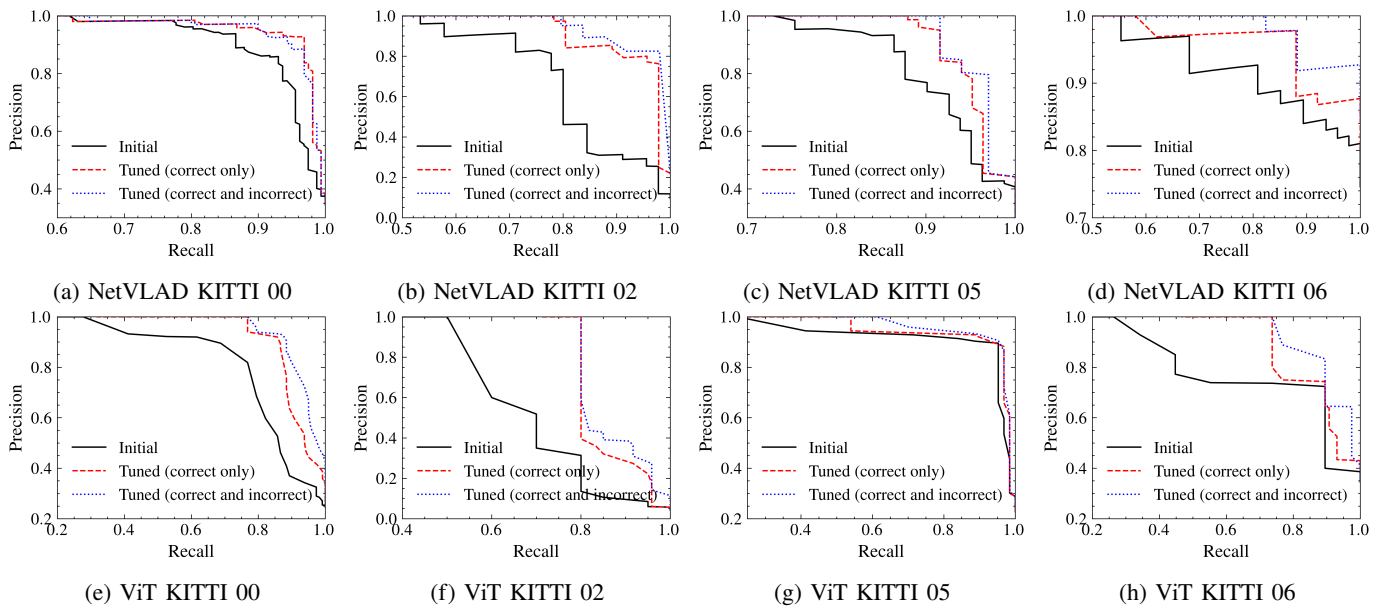


Fig. 4: Precision-Recall performance in loop-closure detection on various KITTI sequences with two different network architecture: NetVLAD [3] and ViT [31]. As expected, we can see that the networks tuned on the KITTI-360-09 sequence achieves better precision and recall on all sequences.

We sum the Kullback-Leibler divergences of the query  $q$  ( $D_{KL}(V_q||T)$ ) and the negative  $n^q$  ( $D_{KL}(V_{n^q}||T)$ ) to obtain the combined loss  $L$  of the incorrect sample  $s \in S_{incorrect}$ ,

$$L = \frac{1}{2} (D_{KL}(V_q||T) + D_{KL}(V_{n^q}||T)) \quad (5)$$

The intuition behind the use of this loss function is to increase the variance estimates of both the query and negative images towards a higher variance without changing their means, since those images are confusing for the VPR system and led to loop closing outliers.

It is important to note that training using uncertainty-aware losses can have detrimental effects on the resulting precision of the place recognition network [14]. However, as we show in the following section, a variance estimator with reasonable performance can be trained on a separate smaller network that can be run cheaply on a CPU. This could allow practitioners

to keep the precision of a conventionally trained VPR network and run a smaller uncertainty estimation network in parallel.

#### IV. EXPERIMENTS

Our experiments are divided into three parts. We first demonstrate the quality of the extracted training tuples by using them to train a network for the task of place recognition from a classification baseline. Second, we demonstrate that we can calibrate a state-of-the-art VPR approach for a target domain using our technique. Third, we show that we can achieve uncertainty estimates tailored to the target environment. All the hyperparameters values used in our experiments can be found in our open-source implementation and correspond to the ones used in [3] and [15].

### A. Training a new VPR System

To show the effectiveness of our approach to produce valuable tuning samples from a calibration run through an environment, we trained a new VPR network based exclusively on the samples extracted from a single KITTI-360 [33] sequence and we tested the resulting VPR network on KITTI [34] sequences. All the sequences were collected in the streets of the same mid-size city. We used the KITTI-360-09 sequence for tuning, and the KITTI-{00, 02, 05, 06} sequences for testing. The testing sequences were collected years apart from the tuning sequence and were selected based on the significant overlaps within their trajectory, which are essential to recognize places.

Our initial model consist of a VGG16 network pretrained on ImageNet [35] for which we replaced the classification head with a randomly initialized NetVLAD pooling layer [3]. To show the generalization of the approach on different network architectures, we also tuned a Vision Transformer (ViT) [31] using the penultimate layer features as descriptors.

The new networks were tuned for place recognition using a triplet margin loss for 10 epochs, which was enough to achieve convergence. The relative poses, loop closures, are estimated with stereo pairs and the SLAM visual odometry is computed and managed using RTAB-Map [36]. Our technique successfully extracted 291 training tuples in  $S_{correct}$ , and 49 in  $S_{incorrect}$ , from the tuning sequence.

To validate the training procedure, we computed the similarity score, based on the  $L_2$  distance between global descriptors, of all pairs of images in KITTI-00 sequence. In Fig. 3, we compared the resulting similarity matrix with the one before tuning and the one obtained with NetVLAD. NetVLAD, which is pretrained on city streets images, is known to achieve high accuracy on the KITTI sequences [37]. We can see that our approach converges to a similar result as NetVLAD, especially in the zones where multiples places are revisited and recognized (i.e., high similarity) near the bottom left and right corners (darker blue). The contrast with negative matches is also accentuated.

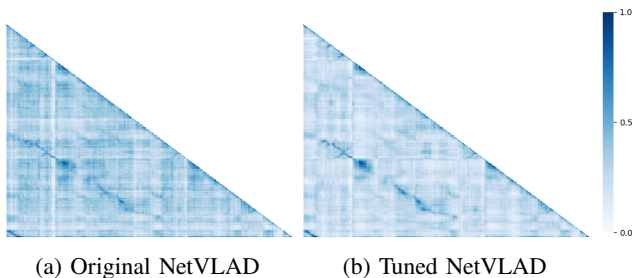


Fig. 5: Self-Supervised domain calibration of a visual-similarity metric. An illustration of the similarity matrix before (Original NetVLAD) and after training (Tuned NetVLAD) compared. As expected, the similarity between positive pairs has increased (blue), and it has decreased between negative pairs (white).

Using the ground truth poses of the KITTI sequences [34], we computed the precision and recall of our VPR system resulting matches before and after tuning, with or without

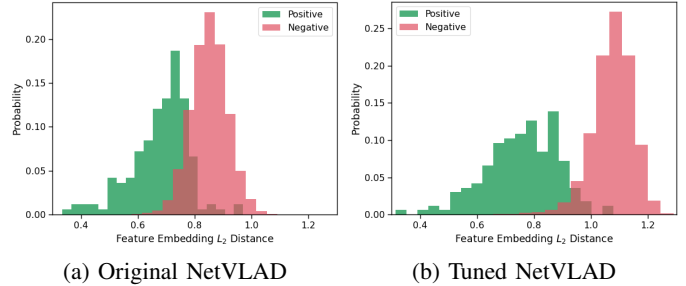


Fig. 6: Separation distance calibration. Histograms of the  $L_2$  distance between the positive pairs (green) and negative pairs (red). As expected, the separation increased between the positive pairs and negative pairs after tuning, making it easier to set a VPR threshold.

TABLE I: Average percentage and standard deviation of correct matches obtained by NetVLAD before and after tuning. We can see that the domain calibration increased the percentage of correct matches and thus the number of loop closures.

	Indoor 1	Indoor 2	Indoor 3
Original NetVLAD	65.4 ± 8.9%	61.7 ± 12.4 %	75.8 ± 5.9 %
Tuned NetVLAD	72.0 ± 8.7%	71.1 ± 10.6 %	82.6 ± 4.8 %

the incorrect matches. The curves in Fig. 4 represent the performance for varying detection threshold values for loop closure detection. A loop closure is considered as detected if the distance between the two images global descriptors is inferior to the threshold, there exists sufficient keypoints matches to compute a relative pose measurement, and it passes the test of robust pose graph optimization. We can see a clear improvement in precision and recall after tuning both NetVLAD and ViT. We also see some small improvements when using the incorrect matches, especially on the KITTI 06 sequence, however we expect the effects of incorrect matches to be greater for initial networks with low precision since it should reduce the number of false positives. While state-of-the-art results were not expected on the well-studied KITTI dataset, we are able to demonstrate the quality and efficiency of the gathered training samples from a single run through the environment without manual labelling or GPS bootstrapping.

### B. Calibration of an Existing VPR system

In this set of experiments, we demonstrate that we can improve the performance of a pretrained state-of-the-art VPR network (NetVLAD [3]) by tuning it to a different target domain. We performed four runs through an indoor office environment (see images in Fig. 1) using an Intel Realsense D455 camera, with multiple overlaps to ensure place recognition. The first run served to extract 166 training tuples, and the three others have been used for testing.

As shown in Fig. 5, we computed the similarity score for each image pairs in the training sequence before (i.e., original pretrained version of NetVLAD on the Pittsburgh dataset [3]) and after tuning. We can observe a significant improvement in contrast between positive and negative matches hinting to a better distinction between them during testing.



Fig. 7: Examples of images with high estimated uncertainty. We can see the presence of under/overexposure and occlusions.

TABLE II: Uncertainty Estimation results on KITTI sequences. We report the  $F_1$  score (computed from precision and recall), the Expected Calibration Error using the cosine similarity between the descriptors as uncertainty estimates ( $ECE_{sim}$ ), and the  $ECE$  using our trained uncertainty estimates ( $ECE_{ours}$ ) for each sequence with 2 different CNN backbone networks. We also indicate the networks size as well as their respective inference time on GPU (NVIDIA RTX3070) and CPU (AMD Ryzen 7).

	KITTI 00			KITTI 02			KITTI 05			KITTI 06			Resources		
	$F_1$ score	$ECE_{sim}$	$ECE_{ours}$	$F_1$ score	$ECE_{sim}$	$ECE_{ours}$	$F_1$ score	$ECE_{sim}$	$ECE_{ours}$	$F_1$ score	$ECE_{sim}$	$ECE_{ours}$	Size (MB)	GPU (s)	CPU (s)
VGG16	0.848	0.774	<b>0.186</b>	0.815	0.801	<b>0.226</b>	0.821	0.769	<b>0.125</b>	0.732	0.802	<b>0.305</b>	82.0	0.004	0.052
MobileNetv3	0.874	0.949	<b>0.242</b>	0.704	0.946	<b>0.150</b>	0.779	0.948	<b>0.197</b>	0.720	0.945	<b>0.367</b>	23.8	0.007	0.015

We corroborate this result in Fig. 6 which shows histograms of the  $L_2$  distance between all pairs of images. The positive pairs are noted in green and the negative ones in red. Confirming the previous result, the separation between the positive and negative pairs is greater after tuning. Fig. 6 shows that our calibration technique is able to fine-tune the VPR network and distort the feature embedding to increase the distance between similar and dissimilar places. This has practical implications for the deployment of VPR systems since the threshold to determine if the distance represents a match becomes easier to set. Moreover, our approach leads to fewer false positives which can be detrimental to the system accuracy and computational performance [11]. In Table I we confirm on the three test sequences that NetVLAD tuned with our technique obtains on average a significantly higher number of correct VPR matches over possible threshold values than its original version (t-test, Bonferroni-corrected,  $p < 1e-5$ ). Therefore, our approach allows practitioners to improve the performance of their VPR system by calibrating its domain through a single run of the environment.

### C. Uncertainty Estimation for VPR

As expected, results in Table II show that training a network explicitly for uncertainty estimation performs better than directly using the cosine similarity between descriptors as a confidence measure. Also, we noticed that training with an uncertainty loss does not provide as much improvement in precision and recall as the triplet margin loss. However, having uncertainty estimates is preferable in safety critical applications. One could even combine a network trained for state-of-the-art precision and another trained for uncertainty in the same system if the computing resources are sufficient. To that end, we show that we can achieve reasonable results in uncertainty estimation with a smaller backbone network (MobileNetv3 [38]) which can be run in real-time on a CPU. This decoupling offers flexibility for practical deployments of uncertainty-aware visual place recognition.

In Fig. 7, we present some examples of images with high estimated uncertainties by our technique. The uncertain images are under/overexposed and have occlusions, such that very few useful visual features and keypoints could be extracted from them in order to successfully compute 3D registration.

To measure the accuracy of the uncertainty estimates, we use the *Expected Calibration Error* (ECE), commonly used for classification tasks [39], which computes how well the uncertainty estimates correspond to the model’s precision,

$$ECE = \sum_{m=1}^M \frac{|B_m|}{n} |\text{mAP@1}(B_m) - \text{conf}(B_m)|. \quad (6)$$

As in [16], we compute this metric by dividing the uncertainty estimates into  $M$  equally spaced bins  $B_m$  with corresponding uncertainty level  $U(B_m)$ . For each bin, we compute the precision of the queries it contains,  $\text{mAP@1}(B_m)$ , and compare it with the bin confidence  $\text{conf}(B_m) = 1 - U(B_m)$ . The ECE is low when the high confidence images lead to high precision matches. As expected, the resulting ECEs in Table II are in a similar range as the results presented in the Bayesian Triplet Loss paper [15]. Interestingly for resource-constrained deployments, the smaller MobileNetv3 achieves comparable results to the larger VGG16 while being able to evaluate images in real-time at more than 60Hz on a CPU.

## V. CONCLUSIONS

In this paper, we present a self-supervised method for training and tuning a place recognition neural network leveraging robust SLAM which does not require GPS or ground truth labels for bootstrapping. We demonstrate the efficiency of the method by training a visual place recognition network from a pretrained classification model, using only the training samples extracted by our method. We also show that our technique can improve the accuracy of an existing deep learning-based VPR system by calibrating it to the target environment. In addition, we show that we can train an uncertainty estimation network for place recognition using the extracted samples.

We consider that our approach has practical benefits for the real-world deployment of place recognition systems. It could be used in an online fashion to perform lifelong learning/tuning on the target environment. Our approach has also the potential for data mining of labeled place recognition training samples on any sequential dataset, which could help increased the overall accuracy of VPR networks. Moreover, while we applied our technique to visual sensors, the same approach could be used for other type of sensors used for place recognition (e.g.

lidars). Finally, we believe that leveraging the recent progress in robust SLAM to improve the performance of deep learning based techniques is a promising avenue that could lead to a tighter integration between the two fields of research.

#### REFERENCES

- [1] S. Lowry, N. Sünderhauf, P. Newman, J. J. Leonard, D. Cox, P. Corke, and M. J. Milford, “Visual Place Recognition: A Survey,” *IEEE Transactions on Robotics*, vol. 32, no. 1, pp. 1–19, Feb. 2016.
- [2] T. Barros, R. Pereira, L. Garrote, C. Premevida, and U. J. Nunes, “Place recognition survey: An update on deep learning approaches,” *arXiv:2106.10458 [cs]*, Jun. 2021.
- [3] R. Arandjelović, P. Gronat, A. Torii, T. Pajdla, and J. Sivic, “NetVLAD: CNN Architecture for Weakly Supervised Place Recognition,” *IEEE Transactions on Pattern Analysis and Machine Intelligence*, vol. 40, no. 6, pp. 1437–1451, Jun. 2018.
- [4] S. Hausler, S. Garg, M. Xu, M. Milford, and T. Fischer, “Patch-NetVLAD: Multi-Scale Fusion of Locally-Global Descriptors for Place Recognition,” in *2021 IEEE/CVF Conference on Computer Vision and Pattern Recognition (CVPR)*, Jun. 2021, pp. 14 136–14 147.
- [5] M. Leyva-Vallina, N. Strisciuglio, and N. Petkov, “Generalized Contrastive Optimization of Siamese Networks for Place Recognition,” Mar. 2021.
- [6] J. Yosinski, J. Clune, Y. Bengio, and H. Lipson, “How transferable are features in deep neural networks?” in *Advances in Neural Information Processing Systems*, vol. 27. Curran Associates, Inc., 2014.
- [7] P.-Y. Lajoie, S. Hu, G. Beltrame, and L. Carlone, “Modeling Perceptual Aliasing in SLAM via Discrete–Continuous Graphical Models,” *IEEE Robotics and Automation Letters*, vol. 4, no. 2, pp. 1232–1239, Apr. 2019.
- [8] H. Yang, P. Antonante, V. Tzoumas, and L. Carlone, “Graduated Non-Convexity for Robust Spatial Perception: From Non-Minimal Solvers to Global Outlier Rejection,” *IEEE Robotics and Automation Letters*, vol. 5, no. 2, pp. 1127–1134, Apr. 2020.
- [9] S. Pillai and J. Leonard, “Self-Supervised Visual Place Recognition Learning in Mobile Robots,” *Learning for Localization and Mapping Workshop IROS 2017*, Nov. 2017.
- [10] F. Radenović, G. Toliás, and O. Chum, “Fine-Tuning CNN Image Retrieval with No Human Annotation,” *IEEE Transactions on Pattern Analysis and Machine Intelligence*, vol. 41, no. 7, pp. 1655–1668, Jul. 2019.
- [11] H. Carson, J. J. Ford, and M. Milford, “Predicting to Improve: Integrity Measures for Assessing Visual Localization Performance,” *IEEE Robotics and Automation Letters*, vol. 7, no. 4, pp. 9627–9634, Oct. 2022.
- [12] S. Garg, T. Fischer, and M. Milford, “Where is your place, Visual Place Recognition?” in *Proceedings of the Thirtieth International Joint Conference on Artificial Intelligence*, Aug. 2021, pp. 4416–4425.
- [13] H. Jégou, M. Douze, C. Schmid, and P. Pérez, “Aggregating local descriptors into a compact image representation,” in *2010 IEEE Computer Society Conference on Computer Vision and Pattern Recognition*, Jun. 2010, pp. 3304–3311.
- [14] A. Taha, Y.-T. Chen, T. Misu, A. Shrivastava, and L. Davis, “Unsupervised Data Uncertainty Learning in Visual Retrieval Systems,” Feb. 2019.
- [15] F. Warburg, M. Jørgensen, J. Civera, and S. Hauberg, “Bayesian Triplet Loss: Uncertainty Quantification in Image Retrieval,” in *2021 IEEE/CVF International Conference on Computer Vision (ICCV)*. IEEE Computer Society, Oct. 2021, pp. 12 138–12 148.
- [16] K. Cai, C. X. Lu, and X. Huang, “STUN: Self-Teaching Uncertainty Estimation for Place Recognition,” Mar. 2022.
- [17] C. Cadena, L. Carlone, H. Carrillo, Y. Latif, D. Scaramuzza, J. Neira, I. Reid, and J. J. Leonard, “Past, Present, and Future of Simultaneous Localization and Mapping: Toward the Robust-Perception Age,” *IEEE Transactions on Robotics*, vol. 32, no. 6, pp. 1309–1332, Dec. 2016.
- [18] P.-Y. Lajoie, B. Ramtoula, F. Wu, and G. Beltrame, “Towards Collaborative Simultaneous Localization and Mapping: A Survey of the Current Research Landscape,” *Field Robotics*, vol. 2, no. 1, pp. 971–1000, Mar. 2022.
- [19] F. Wu and G. Beltrame, “Cluster-based Penalty Scaling for Robust Pose Graph Optimization,” *IEEE Robotics and Automation Letters*, vol. 5, no. 4, pp. 6193–6200, Oct. 2020.
- [20] W. Churchill and P. Newman, “Experience-based navigation for long-term localisation,” *The International Journal of Robotics Research*, vol. 32, no. 14, pp. 1645–1661, Dec. 2013.
- [21] P. Mühlfellner, M. Bürki, M. Bosse, W. Derendarz, R. Philippsen, and P. Furgale, “Summary Maps for Lifelong Visual Localization,” *Journal of Field Robotics*, vol. 33, no. 5, pp. 561–590, 2016.
- [22] D. Doan, Y. Latif, T.-J. Chin, Y. Liu, T.-T. Do, and I. Reid, “Scalable Place Recognition Under Appearance Change for Autonomous Driving,” in *2019 IEEE/CVF International Conference on Computer Vision (ICCV)*. IEEE Computer Society, Oct. 2019, pp. 9318–9327.
- [23] A.-D. Doan, Y. Latif, T.-J. Chin, and I. Reid, “HM4: Hidden Markov Model with Memory Management for Visual Place Recognition,” Nov. 2020.
- [24] H. Porav, T. Bruls, and P. Newman, “Don’t Worry About the Weather: Unsupervised Condition-Dependent Domain Adaptation,” in *2019 IEEE Intelligent Transportation Systems Conference (ITSC)*, Oct. 2019, pp. 33–40.
- [25] S. Schubert, P. Neubert, and P. Protzel, “Graph-based non-linear least squares optimization for visual place recognition in changing environments,” *IEEE Robotics and Automation Letters*, vol. 6, no. 2, pp. 811–818, Apr. 2021.
- [26] J. Wen, R. Liu, N. Zheng, Q. Zheng, Z. Gong, and J. Yuan, “Exploiting local feature patterns for unsupervised domain adaptation,” in *Proceedings of the Thirty-Third AAAI Conference on Artificial Intelligence and Thirty-First Innovative Applications of Artificial Intelligence Conference and Ninth AAAI Symposium on Educational Advances in Artificial Intelligence*, ser. AAAI’19/IAAI’19/EAAI’19. Honolulu, Hawaii, USA: AAAI Press, Jan. 2019, pp. 5401–5408.
- [27] H. Hu, Z. Qiao, M. Cheng, Z. Liu, and H. Wang, “DASGIL: Domain Adaptation for Semantic and Geometric-Aware Image-Based Localization,” *IEEE Transactions on Image Processing*, vol. 30, pp. 1342–1353, 2021.
- [28] C. Chen, X. Liu, X. Xu, Y. Li, L. Ding, R. Wang, and C. Feng, “Self-Supervised Visual Place Recognition by Mining Temporal and Feature Neighborhoods,” Aug. 2022.
- [29] A. D. Kiureghian and O. Ditlevsen, “Aleatory or epistemic? Does it matter?” *Structural Safety*, vol. 31, no. 2, pp. 105–112, Mar. 2009.
- [30] B. Zhou, A. Lapedriza, A. Torralba, and A. Oliva, “Places: An Image Database for Deep Scene Understanding,” *Journal of Vision*, vol. 17, no. 10, p. 296, Aug. 2017.
- [31] A. Dosovitskiy, L. Beyer, A. Kolesnikov, D. Weissenborn, X. Zhai, T. Unterthiner, M. Dehghani, M. Minderer, G. Heigold, S. Gelly, J. Uszkoreit, and N. Houlsby, “An Image is Worth 16x16 Words: Transformers for Image Recognition at Scale,” *arXiv:2010.11929 [cs]*, Jun. 2021.
- [32] C. P. Robert, “Intrinsic losses,” *Theory and Decision*, vol. 40, no. 2, pp. 191–214, Mar. 1996.
- [33] Y. Liao, J. Xie, and A. Geiger, “KITTI-360: A Novel Dataset and Benchmarks for Urban Scene Understanding in 2D and 3D,” *IEEE Transactions on Pattern Analysis and Machine Intelligence*, pp. 1–1, 2022.
- [34] A. Geiger, P. Lenz, and R. Urtasun, “Are we ready for autonomous driving? The KITTI vision benchmark suite,” in *2012 IEEE Conference on Computer Vision and Pattern Recognition*. Providence, RI: IEEE, Jun. 2012, pp. 3354–3361.
- [35] K. Simonyan and A. Zisserman, “Very deep convolutional networks for large-scale image recognition,” in *International Conference on Learning Representations*, 2015.
- [36] M. Labbé and F. Michaud, “RTAB-Map as an open-source lidar and visual simultaneous localization and mapping library for large-scale and long-term online operation,” *Journal of Field Robotics*, vol. 36, no. 2, pp. 416–446, 2019.
- [37] T. Cieslewski, S. Choudhary, and D. Scaramuzza, “Data-Efficient Decentralized Visual SLAM,” in *2018 IEEE International Conference on Robotics and Automation (ICRA)*, May 2018, pp. 2466–2473.
- [38] A. Howard, M. Sandler, B. Chen, W. Wang, L.-C. Chen, M. Tan, G. Chu, V. Vasudevan, Y. Zhu, R. Pang, H. Adam, and Q. Le, “Searching for MobileNetV3,” in *2019 IEEE/CVF International Conference on Computer Vision (ICCV)*, Oct. 2019, pp. 1314–1324.
- [39] F. K. Gustafsson, M. Danelljan, and T. B. Schon, “Evaluating Scalable Bayesian Deep Learning Methods for Robust Computer Vision,” in *2020 IEEE/CVF Conference on Computer Vision and Pattern Recognition Workshops (CVPRW)*, Jun. 2020, pp. 1289–1298.